LAWRENCE
LIVERMORE
NATIONAL
LABORATORY

LLNL-JRNL-839659

Low- and high-temperature heat capacity of metallic Technetium

J. N. Zappey, E. E. Moore, O. Benes, J. C. Griveau, R. J. M Konings

September 8, 2022

The Journal of Chemical Thermodynamics

Disclaimer

J. Chem. Thermodynamics 189 (2024) 107200

Contents lists available at ScienceDirect

The Journal of Chemical Thermodynamics

journal homepage: www.journals.elsevier.com/the-journal-of-chemical-thermodynamics

Low- and high-temperature heat capacity of metallic technetium

J.N. Zappey [a,b], E.E. Moore [a,c], O. Beneš [a,*], J.-C. Griveau [a], R.J.M. Konings [a,b]

[a] European Commission, Joint Research Centre (JRC), Karlsruhe, Germany
[b] Delft University of Technology, Mekelweg 15, 2629 JB Delft, The Netherlands
[c] Lawrence Livermore National Laboratory, Material Science Division, 7000 East Ave, USA

ARTICLE INFO

Keywords:
Heat capacity
Technetium
Calorimetry
Enthalpy
Fission product

ABSTRACT

The heat capacity of technetium metal has been measured from 2.1 K to 293 K using relaxation calorimetry and the enthalpy increment up to 1700 K using drop calorimetry. The low-temperature calorimetry measurements revealed a superconducting transition temperature of $T_C = (7.76 \pm 0.08)$ K. The zero-degree Debye temperature (θ_E) and the electronic heat capacity coefficient (γ_e) of the normal state were derived as (307 ± 5) K and (4.22 ± 0.20) mJ·K^{-2}·mol^{-1}, respectively. The standard entropy of the superconducting standard state was derived as $S^\circ_m(298.15) = (36.8 \pm 1.3)$ J·K^{-1}·mol^{-1}. The fitting of enthalpy-increment data together with high-temperature heat capacity data reported in literature yielded a heat capacity equation up to 1700 K.

1. Introduction

Technetium (Tc) is a silver-grey transition metal with low natural abundance [1]. It is, however, one of the major fission product created during nuclear energy generation. Its fission yield is approximately 6 %, ranking amongst the highest of the fission products. Also its half-life ranks among one of the highest of the fission products, 2.1×10^5 years. Technetium can occur in various oxidation states and the oxy-anions of valence states IV, V and VI are quite stable [2,3], and some are relatively mobile in an oxidising aqueous environment [4]. This makes technetium of major concern during both energy production as well as high-level waste storage [5].

In irradiated nuclear fuel the oxygen potential is low, and technetium remains in metallic state. It is a component of the 5-metal particles, a fission product alloy of Ru-Pd-Rh-MoTc, which are found throughout the nuclear fuel [6,7] and are very stable, even surviving the fuel reprocessing in nitric acid. The stability of these 5-metal particles is generally modelled by computational chemical thermodynamic methods [8], which require accurate description of the lattice stability of the constituent elements. It is therefore necessary to have a accurate knowledge of both low- and high-temperature thermophysical properties. Since there is little to no information available of the technetium metal, previous assessments [9–11] have heavily relied on estimates and extrapolations of what is known. These estimates are made with sound scientific basis in mind using comparisons to other transition metals, particularly the neighboring Ru, Rh and Os metals, which have a hexagonal closepacked (A3) crystal structure, similar to technetium.

Thermophysical properties such as the heat capacity across a wide temperature range provide information on phase transitions, lattice vibrations, energy excitations as well as electronic properties. In recent years various studies have been performed on heat capacity and enthalpy increments of technetium metal. Experimental data exist between the temperature 3 and 15 K [12] and between 323 and 1500 K [13,14]. In the range of 15 K to 323 K no experimental data exist, and data needs to be interpolated or estimated, in order to obtain the standard entropy, a key thermodynamic parameter. One of the reasons to perform experimental studies on lower temperature heat capacity is that the entropy Debye temperature model loses its validity under 100 K leading to uncertainty in the calculated S°_m values. In this study, we aim to fill this gap.

2. Materials and experimental methods

2.1. Sample preparation

The technetium metal was taken from the batch that was produced by Spirlet and coworkers, as described in [15]. The metal was obtained by reducing ammonium pertechnetate in Ar/H_2 in a resistance furnace at 1073 K. The metallic powder was remelted several times into small buttons by arc melting to improve the purity of the material by evaporating the impurities. Finally the metal was casted into rods that were cut to cylinders of required size. The microstructure of the rods consisted

* Corresponding author.
E-mail address: ondrej.benes@ec.europa.eu (O. Beneš).

https://doi.org/10.1016/j.jct.2023.107200
Received 31 July 2023; Received in revised form 25 October 2023; Accepted 25 October 2023
Available online 30 October 2023

of large grains often extending from the centre to the rim of the rods [15]. Three analysis performed on the final ingots produced at that time show a purity of 99.819 % to 99.982 %, with main impurities W (~1000 ppm), Ce (~800 ppm), Re (~450 ppm), Si (~220 ppm) and (Pu + U) (~210 ppm). The oxygen content was found between 44 and 187 ppm.

The current samples were obtained from the remaining cutoff pieces, which have been stored in a closed contained in a glove box with controlled atmosphere. Rectangular pieces of technetium metal were prepared from the larger piece of metal using a diamond saw. Since the thermal coupling between sample and sapphire platform of the measurement device (puck [16]) is improved on case of a clean and flat surface, the sample for low-temperature measurements was polished afterwards and remained shiny at all time.

2.2. Low-temperature heat capacity measurements

The low-temperature heat capacity measurements were performed by relaxation calorimetry on a sample of 10.77 mg, annealed before the measurement, using a Physical Property Measurement System (PPMS-9, Quantum Design). The heat capacity contribution arising from the platform, wires and Apiezon-N grease that were used has been determined via the addenda protocol. The measurements covered a temperature range of 2.1 K to 293 K and was performed both in the absence of magnetic field and with applied value of B = 1 T, the latter to suppress the superconducting transition, in order to determine the standard entropy more easily. The final uncertainty was estimated to be 2 %. A more detailed description of the technique and details of the instrument can be found in [16]. Correction for self-heating of the sample due to beta decay was not necessary, in view of the small mass in combination with the low heat production (15 μW/g for ^{99}Tc).

The low-temperature heat capacity was fitted for two different temperature regimes. At very low temperatures (less than 20 K) a harmonic-lattice model [17] was used as indicated in the following equation, where n = 3,5,7,9:

$$C_{lat} = \gamma T + \sum B_n T^n \tag{1}$$

In this equation γ is the electronic heat capacity coefficient.

At temperature above 20 K, the Debye and Einstein models were used which is represented by the following equation [18–20]:

$$Cp,m = n_D D(\Theta_D) + n_{E1} E(\Theta_{E1}) + n_{E2} E(\Theta_{E2}) \tag{2}$$

Here the parameters $D(\Theta_D)$, $E(\Theta_{E1})$ and $E(\Theta_{E2})$ are the Debye function, low- and high-temperature Einstein functions respectively, which are defined in Eq. (3) and (4). n_D, n_{E1} and n_{E2} are adjustable parameters whose sum should equal the number of atoms in a formula unit (i.e. 1 for elemental technetium) and Θ_D, Θ_{E1} and Θ_{E2} are the corresponding Debye and Einstein temperatures. In both equations (3) and (4), $x = \Theta_D/T$ and $x = \Theta_E$.

For the Debye and Einstein functions, respectively.

$$D(\theta_D) = 9R\left(\frac{1}{x}\right)^3 \int_0^x \frac{e^x x^4}{(e^x-1)^2} dx \tag{3}$$

$$E(\theta_{En}) = 3Rx^2 \frac{e^x}{(e^x-1)^2} \tag{4}$$

2.3. High-temperature enthalpy increment measurements

The high-temperature enthalpy increment $\Delta^T_{298.15K}H^\circ$ was measured using a Setaram Multi Detector High Temperature Calorimeter operated in drop mode. Before the study, the temperature recording of the calorimeter detector was calibrated using high purity (≥99.95 %) standard materials representing fixed points of the ITS-90 Scale, i.e. In, Zn, Pb, Al, Ag and Au [21]. The temperature uncertainty of the measurement was estimated to be 2 K according to the Setaram manufacturer's specifications. Per round of experiment three to four solid pieces of technetium-metal were measured, with a weight ranging from 40 to 70 mg. Before the study, these samples were annealed for 4 h at 1400 K to remove any radiation damage that might have occurred during their storage.

The experiments were performed between 473 K and 1773 K with steps of 100 K. During the study a high purity argon (5 N) was used as a carrier gas, to protect the samples from oxidation. Moreover, the calorimeter was installed in a glove box with a argon atmosphere connected to a purifier, which resulted in concentrations of oxygen and water in the parts-per-million range.

After the samples were introduced into the sample holder of the instrument, the heating program started and the calorimeter stabilized at the desired temperature in 7 h. After this initial heating time the samples were dropped from the sample holder (ambient temperature) into detector with a 25 min time interval. The 25 min interval proved sufficient to re-stabilise the temperature and the heat flow for the following drop.

In order to determine the sensitivity of the detector a reference, MgO, was placed before and after each sample. The sensitivity of the device was determined using the following equation:

$$S = \frac{\int \phi_r dt}{\int_{T_a}^{T_m} C_{p,r}(T) dt} \cdot \frac{M_r}{m_r} \tag{5}$$

In this equation the first integral $\phi_r dt$ is the heat flow integrated with respect to time. T_a is the ambient temperature and T_m is the recorded temperature of sample. $C_{p,r}(T)dt$ is the heat capacity function of the reference material [22]. M_r and m_r represent the molar mass of the reference and the weight of the reference material. The reference

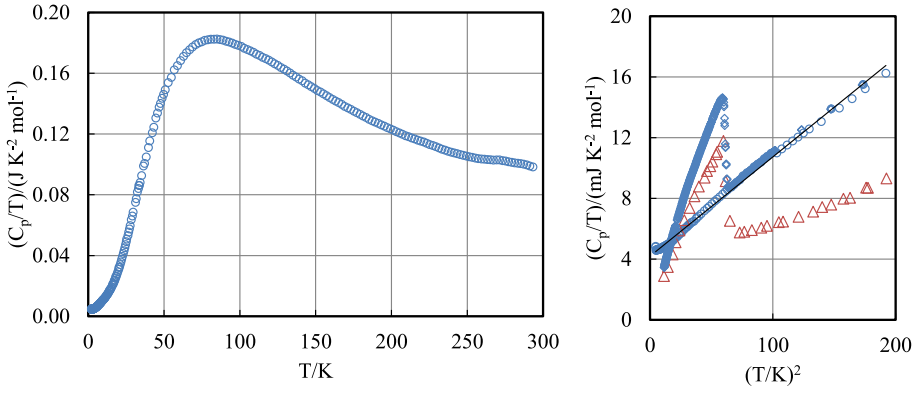

Figure 1. The low-temperature heat capacity of technetium metal. Left: C_p/T vs. T of the normal state as measured at B = 1 T. Right: C_p/T vs. T^2 the superconducting state measured at B = 0 T and comparison with experiment results of Trainor and Brodsky [12] shown by red triangles. (For interpretation of the references to colour in this figure legend, the reader is referred to the web version of this article.)

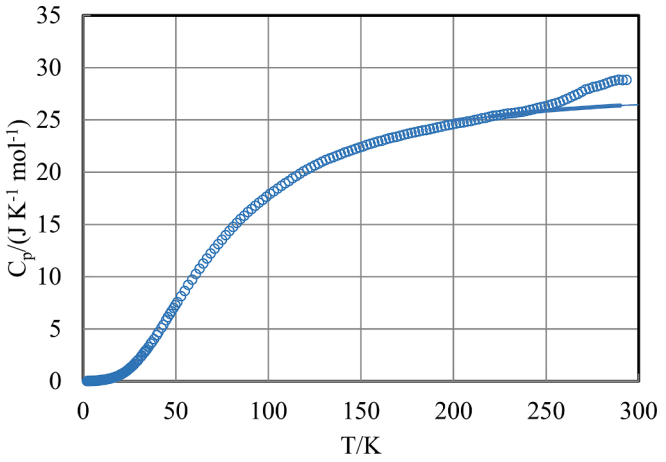

Figure 2. Measured low-temperature heat capacity for the normal state of technetium metal from 2.1 − 293 K in a magnetic field of B = 1 T. The solid line show the extrapolation to T = 298.15 K.

samples weighed between 50 mg and 150 mg.

The device measures the energy that is needed to heat up the sample from ambient temperature until the programmed temperature, also known as molar enthalpy increment. The molar enthalpy increment is calculated according to equation (6):

$$\Delta_{T_a}^{T_m} H_m = \frac{\int \phi_S dt}{S} \cdot \frac{M_s}{m_s} \tag{6}$$

in which $\int \phi_S dt$ is the time integral of the energy provided to bring the sample at the programmed temperature, S is the sensitivity which is obtained as the average of two reference materials dropped before and after the sample and is calculated from equation (5), M_s is the molar mass of the sample and m_s is the mass of the sample. From these measurements it is possible to derive the enthalpy and heat capacity of the material using the equation:

$$C_p = \frac{\partial H}{\partial T_p} \tag{7}$$

where C_p is the heat capacity of the sample, $\partial H/\partial T_p$ is the derivative of the enthalpy function with respect to T at constant pressure.

3. Results and discussion

3.1. Low-temperature heat capacity and standard entropy

The low-temperature heat capacity was measured between 2 K and 293 K in two runs: a run of the complete temperature range in a field of B = 1 T to suppress the superconducting state, and a run between 2.1 and 45 K without an applied magnetic field. The results of the measurements can be found in the Appendix.

In absence of a magnetic field, the superconducting transition was observed with a peak T_C = (7.76 ± 0.08) K, as shown in Figure 1 (right). The uncertainty is taken as approximately twice the temperature interval in the measured range. In the magnetic field of B = 1 T the superconducting transition was absent (Figure 1 (left) and Figure 2). However, above approximately 250 K an anomalous increase occurred in the heat capacity, which we consider an experimental artefact resulting from the thermal grease [23–25] and possibly poor thermal coupling between sample and platform. As we will discuss below, the region up to 298.15 K has therefore been extrapolated yielding $C_{p,m}^{\circ}$ = (26.5 ± 1.0) J·K^{-1}·mol^{-1} at T = 298.15 K. The uncertainty is an conservative estimate based on the goodness of the fit, the reported accuracies of standards in literature, and our experience of the effect of the Stycast encapsulation [16,26]. The very low-temperature heat capacity

Table 1
Summary of fitting parameters of the heat capacity of technetium (B = 1 T).

Harmonic lattice-model		Debye-Einstein fit	
Temp. range/K	2–14	Temp. range/K	10–293
γ/J·K^{-2}·mol^{-1}	0.00422	n_D/mol	0.9856
$B3$/J·K^{-4}·mol^{-1}	4.9546 × 10^{-5}	Θ_D	296.53
$B5$/J·K^{-6}·mol^{-1}	5.7988 × 10^{-7}	n_{E1}/mol	0.1046
$B7$/J·K^{-8}·mol^{-1}	−5.3104 × 10^{-9}	Θ_{E1}	633.98
$B9$/J·K^{-10}·mol^{-1}	1.4114 × 10^{-11}	n_{E2}/mol	0.0595
		Θ_{E2}	167.09
		$n_D + n_{E1} + n_{E2}$	1.1497

below 20 K (2–14 K) was fitted with the harmonic model using 4 terms using Eq. (1), for which the parameters are listed in Table 1. The lattice contribution was fitted using Eqs. (2)–(4) for temperatures above 10 K and the results are given in Table 1; it is to be noted that the Debye temperature fit using this model is given as 296.5 K. The data at low temperature were also linearly fitted (R^2 factor = 0.9960) to obtain the Debye temperature (Θ_D) and the electronic heat capacity coefficient (γ_e), where the former is the slope of the plot C_p/T vs. T^2 and latter is the y-intersect of the plot. The zero-degree Debye constant and electronic heat capacity coefficient obtained in this study were (313 ± 5) K and (4.22 ± 0.20) mJ·K^{-2}·mol^{-1}.

Figure 2 depicts a plot of C_p vs. T. The integration of the C_p/T curve allows for the calculation of the standard entropy, which was found S_m° (298.15 K) = (36.8 ± 1.3) J·K^{-1}·mol^{-1} for the normal state. A fitting with polynomials yields almost the same value. The contribution of the entropy of the superconducting transition is negligible, $S_{trs.}$ = 0.004 J·K^{-1}·mol^{-1}.

This value is somewhat different from that recommended in the OECD-NEA TDB review of 1999 [11], S_m° (298.15) = (32.5 ± 0.7) J·K^{-1}·mol^{-1}, based on a physical model by Guillermet and Grimvall [9] describing the vibrational and electronic contributions to the entropy.

Low-temperature heat capacity measurements for technetium metal were reported by Trainor and Brodsky [12] in the 1970 s. They measured it using a pulse heat method [27] in the temperature range from 3 to 15 K. The right graph in in Figure 1 depicts the measurements range that is comparable with the experimental data from Trainor and Brodsky [12]. The comparison shows the following:

- The temperature (peak) of the superconducting transition, (7.76 ± 0.08) K, is slightly lower than that reported by Trainor and Brodsky [12], (7.86 ± 0.01) K. However, the latter value is not the peak value (which is 7.74 K, as extracted from the digitized graph in their work), but obtained from integration of the C_p curves of the superconducting and normal states, which explains the much smaller error compared to their applied temperature increment (0.1–0.3 K in the range of the transition). Other values reported in literature are 7.77 by Sekula et al. [28], and 7.46 K by Kostorz and Mihailovich [29], the latter measured on a sample of significant lower purity. • The width of the transition in our work is very comparable to that found by Trainor and Brodsky [12].
- The electronic heat capacity coefficient γ_e for the normal state of technetium obtained in this study is (4.22 ± 0.20) mJ·K^{-2}·mol^{-1}, which agrees very well with the value by Trainor and Brodsky [12], (4.30 ± 0.05) mJ·K^{-2}·mol^{-1}. • The zero-degree Debye constant from our work, 313 K, is, however, significantly lower compared to the result of Trainor and Brodsky [12], 454 K.
- If we look at Figure 1, we see that the largest deviation between our results and those of Trainor and Brodsky [12] occur for the heat capacity of the normal state just after the transition; our results being significantly higher.

The discrepancy between the two experiments could be due to a number of reasons. First, different impurity levels of our technetium metal compared to Trainor and Brodsky [27]. However, these authors do

Table 2
Enthalpy increment $\Delta^{T}_{298.15K}H^{\circ}$ of technetium metal; δH is the standard deviation and n is the number of samples dropped in a single experiment.

Tm (K)	n	$\Delta^{T}_{298.15K}H$ / (kJ·mol^{-1})	δH	$\frac{\Delta^{T}_{298.15K}H^{\circ}}{T-298.15}$ (J·K^{-1}mol^{-1})
429	3	3.33	0.04	25.71
584	3	8.31	0.09	29.33
703	3	10.52	0.93	26.23
786	3	13.40	0.69	27.72
887	3	14.74	0.62	25.27
988	3	17.48	0.22	25.58
1087	4	19.69	1.49	25.19
1188	4	22.63	0.97	25.66
1291	4	28.22	2.65	28.69
1392	4	29.61	2.13	27.32
1493	4	31.47	0.79	26.58
1594	5	35.12	2.00	27.35
1697	4	36.67	1.89	26.46

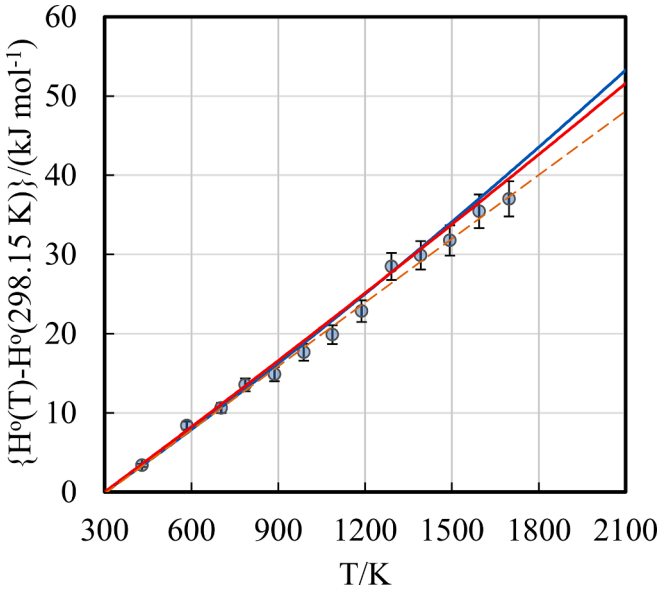

Figure 3. Measured high-temperature enthalpy increment of technetium metal; the red line shows the fitted equation, the blue line the recommendation from the OECD-NEA review of 1999 [11], the orange dashed curve the linear fit of the experimental data. (For interpretation of the references to colour in this figure legend, the reader is referred to the web version of this article.)

not report purity of the metal they used, except the resistance ratio ρ(300 K)/ρ(9 K) = 420, suggesting a low number of lattice imperfections. Second, the ageing effect due to the beta decay of ^{99}Tc (~ 300 keV) should be considered. The electron stopping of the beta radiation is not likely to cause atomic displacements in technetium metal. The ingrowth of the decay product ^{99}Ru in our sample would be in the order of around 140 ppm since metal production in the late 1980 s, and is thus well below the level of the other impurities. Such lattice imperfections (defects, impurities) can lead to an increase low temperature heat capacity in metals as reported by Bevk [30] and thus affect the derivation of Θ_D. Third, the metallurgical history of the sample plays a role. Hulm and Goodman [31] showed by systematic magnetisation measurements of rhenium metal that the temperature and width of the superconducting transition is clearly influenced by the metal preparation method and subsequent treatments such as grinding and annealing, causing strong deviations from ideal superconducting behaviour and partially frozen-in magnetic moments. This was attributed to crystalline imperfections and strain. Also here a comparison between the samples is difficult. In both studies they were cut from rods, but details for the Trainor and Brodsky sample are lacking. Finally, differences in the measurement techniques could play a role. Trainor and Brodsky [27] used heat-pulse calorimetry, with the decay heat of the technetium samples as heating source, implying that the measurement started at cryogenic temperature. In the PPMS instrument used in this study the measurement is performed from room temperature down to cryogenic temperature, which means that the results just above the superconducting transition are not affected by the transition kinetics. Also the temperature increment in our work is significantly smaller than in the work of Trainor and Brodsky [27] (see the symbol density in the right graph of Figure 1).

3.2. High-temperature enthalpy increment and heat capacity

To determine the high-temperature heat capacity the enthalpy increments for the technetium metal samples were measured between 429 K and 1697 K. The results are reported in Table 2. The table sums the temperature at which a measurement was performed T_m, the number of measurements that were done n, and the mean value of the enthalpy obtained with the corresponding standard deviation (1σ). A graphical representation of the enthalpy increments is found in Figure 3. For each measured temperature the corresponding enthalpy increment value represents the mean of all performed measurements at that temperature.

To the best of our knowledge, these are the first experimental enthalpy increment data for technetium metal. Experimental data on the heat capacity of technetium metal is less scarce in literature but the results scatter considerably. Shirasu and Minato [13] measured the heat capacity of technetium metal between 323 K and 1073 K using differential scanning calorimetry. Their measurements confirmed the earlier results of the physical model by Rard et al. [11], who derived the heat capacity using the temperature dependent entropy Debye temperature and revised thermodynamic data of rhenium. This approach was basically similar to the one of Guillermet and Grimvall [9], however, the thermodynamic data they used was older. Another study of the heat capacity of technetium metal was conducted by van der Laan and Konings [32], however their heat capacity was basically an estimation. In that study they measured the heat capacity of an irradiated technetium metal sample that had a composition 15 % ruthenium and 85 % technetium after the irradiation. To derive the heat capacity of

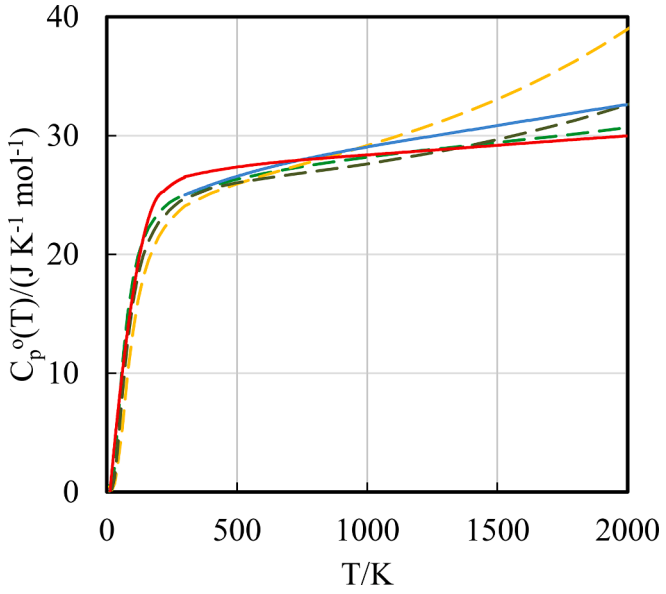

Figure 4. The high-temperature heat capacity of technetium metal; the red line shows the fitted equation, the blue line the recommendation from the OECD-NEA review of 1999 [11,37]. Also shown are the recommended curves for rhenium (light green), ruthenium (yellow) and osmium (dark green). (For interpretation of the references to colour in this figure legend, the reader is referred to the web version of this article.)

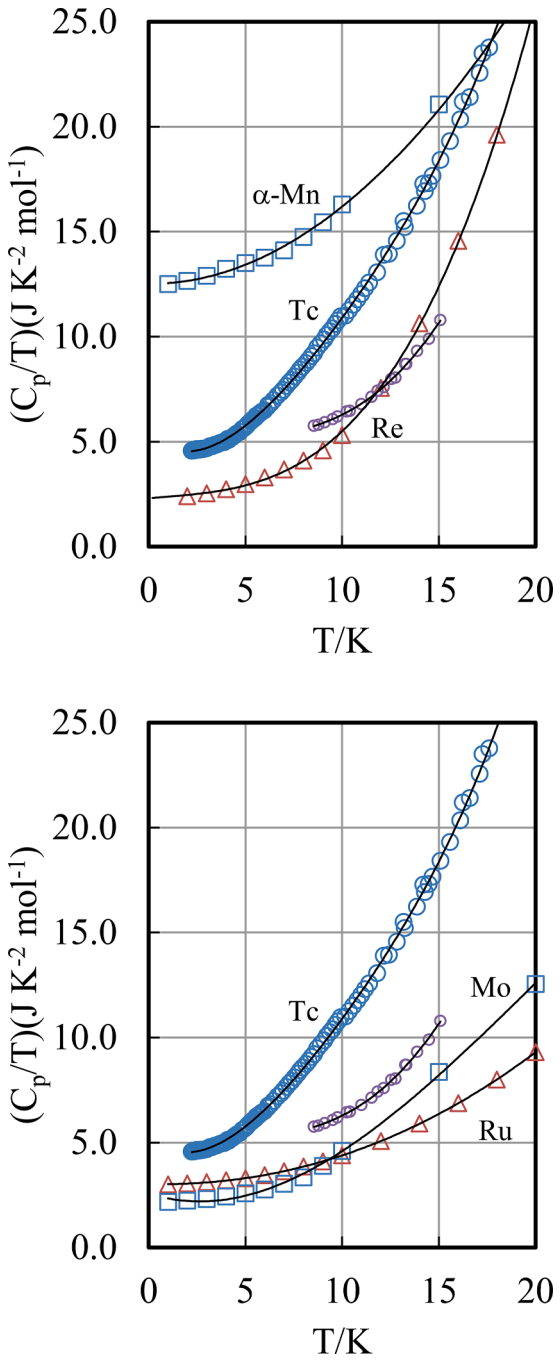

Figure 5. The low-temperature heat capacity of the metals in group (7) (top) and of the Mo-Tc-Ru suite in the second d-block series (bottom) of the periodic table of elements. The blue circles represent the results from the current study, the small magenta circles those of Trainor and Brodsky [27]. (For interpretation of the references to colour in this figure legend, the reader is referred to the web version of this article.)

technetium they applied the Neumann-Kopp rule on the data they found for their alloy. For this estimation they had to do two assumptions namely, that the irradiation-induced heterogeneity of the sample did not affect the heat capacity and that there is no heat capacity change from forming the alloy. The validity of the latter assumption was confirmed by the results of Shirasu and Minato [13] for a $Tc_{0.51}Ru_{0.49}$ alloy. Finally, Spitsyn et al. [14] reported measurements of the heat capacity at higher temperatures (950 to 1580 K).

The enthalpy increment data clearly suggest that the heat capacity of technetium does not change substantially in the measured temperature range, evident from the fact that the apparent heat capacity $\Delta^{T}_{298.15K}H°/(T - 298.15)$ is fairly constant, as can be seen in Table 2. The results suggest an average value 26.7 $J{\cdot}K^{-1}{\cdot}mol^{-1}$, so in very good agreement with the low temperature result at $T = 298.15$ K.

The recommended high-temperature enthalpy increment equation was obtained by least square fitting a polynomial curve to the collected enthalpy data points as well as with the heat capacity data from Shirasu and Minato [13] in the 300 to 1000 K range, from 1000 to 1600 K Spitsyn et al. [14], and constrained to the value at $T = 298.15$ K:

$$\left\{H^{\circ}_{m}(T) - H^{\circ}_{m}(298.15{\cdot}K)\right\}/\left(J{\cdot}mol^{-1}\right) = 26.9187 \times (T/K) + 0.7686{\cdot}10^{-3} \times (T/K)^{2} + 7.7960{\cdot}10^{4} \times (T/K)^{-1} - 8355.6$$

The overall standard deviation of the fit is $\sigma = 1.303$, composed of $\sigma = 1.596$ for the enthalpy increments and 1.009 for the heat capacity values.

As can be seen in Figure 3, this equation describes the enthalpy data well; it is slightly above the simple linear fit of the enthalpy increment data and just below the enthalpy curve from OECD/NEA TDB review. Figure 4 shows the derived heat capacity in the range 0 to 2000 K as together with the curve from OECD/NEA TDB review [11]. In this case the difference is more significant. First of all, a substantial difference exists for the values at room temperature, which is $C^{\circ}_{p,m}(298.15\ K) = 24.88\ J{\cdot}K^{-1}{\cdot}mol^{-1}$ in the OECD/NEA TDB review value, lower than the value $C^{\circ}_{p,m}(298.15\ K) = (26.5 \pm 1.0)\ J{\cdot}K^{-1}{\cdot}mol^{-1}$ found here. Second, at higher temperatures the curve from our work shows only a moderate increase of the heat capacity compared to that from the OECD/NEA TDB recommendation, in line with our observation that the apparent heat capacity $\Delta^{T}_{298.15K}H°/(T - 298.15)$ is fairly constant in the temperature range up to 1700 K, the upper limit of our measurements.

3.3. Comparison to neighbouring d-block metals

It is interesting to compare the heat capacity of technetium to that of the neighboring elements in the periodic table of elements which have similar electronic and chemical charateristics. These are the hcp metals Ru and Re and the bcc metals Mn and Mo. We have also included capacity Fe and Os in the comparison to complete groups 7 and 8 of the periodic table. The data used for these elements have been taken from the reviews for Ru, Re and Os by Arblaster [33–35], and Mn and Mo by Desai [36]

The low-temperature heat capacity curves of the metals in the group (7) are shown in Figure 5. In this group, all metals have a $(n\text{-}1)s^2nd^5$ electron configuration. It can be seen that the heat capacity of technetium derived from the current results is in between α-Mn (bcc) and Re (hcp), whereas that derived from the results of Trainor and Brodsky [27] is identical with Re. Also shown in Figure 2 is the comparison with the neighbouring elements in the second *d*-block series, which shows significantly higher heat capacity for technetium derived from our results, and only slightly higher for the values of Trainor and Brodsky [27]. However, in this case the $4d^55s^2$ electron configuration of Tc is not the same as Mo $4d^55s^1$ or Ru ($4d^75s^1$). Moreover, Mo has a different crystal structure (bcc).

Figure 4 compares the obtained high-temperature heat capacity curves of Tc to the hcp metals Re, Ru and Os. It can be seen that the heat capacity of technetium is very close to those of Re and Os, all staying close to the Dulong-Petit limit of $3nR$ above room temperature. Ruthenium, in contrast, shows a much stronger increase in the heat capacity at high temperature.

4. Conclusions

- The results for the heat capacity of technetium below T = 20 K obtained in this work, show the superconducting transition (peak) temperature of $T_C = (7.76 \pm 0.08)$ K, in good agreement with

Table A3
Low-temperature heat capacity values obtained for normal state of.

T_m/K	C_p/(J · mol^{-1}·K^{-1})	T_m/ K	C_p/(J·mol^{-1}·K^{-1})	T_m / K	C_p/(J·mol^{-1}·K^{-1})	T_m/K	C_p/(J·mol^{-1}·K^{-1})
2.13	0.0102	7.7	0.0638	33.24	2.7922	155.21	22.718
2.15	0.0104	7.83	0.0661	33.49	2.8825	157.22	22.816
2.23	0.0102	7.95	0.0681	33.76	2.9035	159.23	22.932
2.27	0.0104	8.14	0.0712	34.26	3.017	161.24	23.014
2.3	0.0106	8.27	0.0736	35.25	3.2627	163.24	23.122
2.34	0.0108	8.41	0.0763	36.54	3.6124	165.24	23.24
2.38	0.0109	8.55	0.0788	37.27	3.749	167.24	23.317
2.41	0.0111	8.71	0.0826	38.28	4.0142	169.25	23.385
2.44	0.0113	8.89	0.0861	39.79	4.4179	171.26	23.494
2.48	0.0115	9.07	0.0894	40.61	4.6847	173.26	23.585
2.52	0.0117	9.21	0.0928	42.32	5.1084	175.26	23.662
2.6	0.012	9.37	0.0961	43.33	5.3917	177.27	23.764
2.67	0.0124	9.51	0.0988	44.71	5.8325	179.27	23.817
2.7	0.0126	9.65	0.1024	45.72	6.1177	181.28	23.905
2.71	0.0126	9.78	0.1053	46.84	6.4462	183.28	23.975
2.75	0.0128	9.93	0.1089	47.7	6.6795	185.29	24.027
2.78	0.0129	10.16	0.1117	48.84	7.0075	187.3	24.101
2.82	0.0131	10.36	0.1166	49.82	7.2775	189.3	24.198
2.89	0.0135	10.57	0.1217	50.84	7.5762	191.31	24.282
2.93	0.0137	10.78	0.127	52.82	8.124	193.32	24.345
3.01	0.0141	10.98	0.1322	54.92	8.6305	195.33	24.435
3.08	0.0146	11.18	0.1376	56.81	9.2133	197.34	24.498
3.16	0.0151	11.39	0.1432	58.89	9.7143	199.34	24.577
3.2	0.0153	11.81	0.1542	60.91	10.252	201.34	24.656
3.24	0.0155	12.15	0.1688	62.91	10.764	203.35	24.713
3.28	0.0157	12.42	0.1732	64.91	11.262	205.36	24.764
3.39	0.0164	12.83	0.1869	66.92	11.737	207.36	24.845
3.46	0.0168	13.18	0.2043	68.92	12.215	209.36	24.884
3.5	0.017	13.24	0.2015	70.93	12.683	211.37	24.981
3.58	0.0175	13.86	0.2251	72.93	13.12	213.38	25.047
3.67	0.0181	14.2	0.2455	74.93	13.54	215.37	25.151
3.74	0.0185	14.27	0.2417	76.94	13.975	217.38	25.204
3.82	0.019	14.47	0.2506	78.95	14.364	219.38	25.295
3.9	0.0194	14.67	0.2591	80.96	14.767	221.38	25.38
3.97	0.02	15.09	0.2779	82.96	15.131	223.38	25.433
4.01	0.0202	15.58	0.301	84.97	15.505	225.37	25.471
4.09	0.021	16.1	0.3277	86.98	15.835	227.38	25.543
4.13	0.021	16.24	0.3442	88.99	16.176	229.37	25.62
4.21	0.0217	16.6	0.3555	90.99	16.47	231.37	25.64
4.33	0.0226	17.11	0.3859	92.99	16.793	233.38	25.671
4.41	0.0233	17.26	0.4057	95	17.083	235.39	25.745
4.49	0.024	17.6	0.4184	97	17.359	237.39	25.784
4.56	0.0246	18.13	0.4547	99.01	17.653	239.39	25.856
4.72	0.0258	18.27	0.4763	101.01	17.945	241.4	25.948
4.84	0.0271	18.61	0.4914	103.02	18.172	243.39	26.036
4.92	0.0278	19.14	0.5322	105.03	18.433	245.39	26.124
5	0.0285	19.62	0.5747	107.03	18.692	247.39	26.219
5.07	0.0292	20.15	0.6215	109.04	18.941	249.39	26.29
5.14	0.03	20.31	0.6502	111.05	19.153	251.39	26.374
5.27	0.0314	20.64	0.6699	113.06	19.408	253.38	26.497
5.35	0.0322	21.16	0.72	115.07	19.618	255.38	26.6
5.42	0.033	21.66	0.7738	117.07	19.861	257.38	26.696
5.51	0.0338	22.16	0.8312	119.08	20.08	259.38	26.86
5.57	0.0347	22.67	0.891	121.09	20.273	261.38	27.008
5.63	0.0352	23.17	0.9558	123.09	20.457	263.38	27.172
5.71	0.0361	23.68	1.0205	125.1	20.656	265.38	27.346
5.79	0.037	24.18	1.0907	127.11	20.822	267.37	27.485
5.87	0.0378	24.69	1.1632	129.12	21.002	269.38	27.702
5.98	0.0388	25.19	1.2375	131.12	21.171	271.37	27.908
6.15	0.041	25.42	1.2899	133.13	21.323	273.37	27.996
6.18	0.0417	26.21	1.3926	135.14	21.444	275.36	28.127
6.31	0.0431	26.7	1.4781	137.15	21.588	277.36	28.196
6.46	0.0451	27.21	1.5649	139.16	21.717	279.36	28.303
6.66	0.0479	27.72	1.6548	141.16	21.878	281.35	28.401
6.83	0.0502	28.44	1.8078	143.17	21.973	283.35	28.547
6.95	0.0519	29.24	1.9276	145.17	22.113	285.35	28.677
7.11	0.0544	29.73	2.0351	147.17	22.236	287.34	28.771
7.27	0.0568	31.25	2.3432	149.18	22.362	289.34	28.836
7.39	0.0587	31.74	2.455	151.19	22.466	291.33	28.811
7.54	0.0611	32.48	2.6548	153.2	22.606	293.41	28.825

literature [27]. However, the heat capacity of the normal state just above the transition differs somewhat from the values reported in the only other study reported in literature [27]. Our results indicate that the heat capacity of technetium at very low temperatures is in between the neighboring elements Mn (bcc) and Re (hcp) in group (7) of the periodic table of elements, the literature results are almost identical with Re. New measurements would be needed to resolve this discrepancy, addressing the possible causes identified (defect, impurities, strain).

- Compared to the recommendation in the OECD/NEA TDB review [11,37], the derived thermodynamic properties $C_{p,m}^{\circ}$ and S_m° at T = 298.15 K are somewhat different.
- Above room temperature the derived heat capacity curve is in line with the other hcp metals in groups 7 and 8 of the of the periodic table of elements, slightly lower than the recommendation in the OECD/NEA TDB review [11,37].

Declaration of Competing Interest

The authors declare that they have no known competing financial interests or personal relationships that could have appeared to influence the work reported in this paper.

Data availability

Data will be made available on request.

Acknowledgements

The authors wish to acknowledge the help of Davide Robba for cutting and polishing the sample and Anna Smith for data analysis. The contribution of EEM was in part prepared at LLNL under Contract DE-AC52-07NA27344.

Appendix A. Experimental heat capacity data

References

[1] K. Schwochau, Technetium: Chemistry and Radiopharmaceutical Applications, WILEY-VCH Verlag GmbH, 2000.
[2] C.L. Rulfs, R.A. Pacer, R.F. Hirsch, J. Inorg. Nucl. Chem. 29 (1967) 681–691, technetium metal.
[3] S. Bauters, A.C. Scheinost, K. Schmeide, S. Weiss, K. Dardenne, J. Rothe, N. Mayordomo, R. Steudtner, T. Stumpf, U. Abram, S.M. Butorin, K.O. Kvashnina, Chem. Commun. 56 (2020) 9608–9611.
[4] F. Chen, P.C. Burns, R.C. Ewing, J. Nucl. Mater. 278 (2000) 225–232.
[5] K. Yoshihara, in: Technetium in the Environment, Springer, Berlin Heidelberg, 1996, pp. 17–35.
[6] H. Kleykamp, J. Nucl. Mater. 131 (1985) 221–246.
[7] R. J. M. Konings, T. Wiss, and C. Gueneau. Chapter 34, 2113–2224. L. R. Morss and N. Edelstein and J. Fuger and J. J. Katz, (Ed.), Springer Verlag, (2010).
[8] M.H. Kaye, B.J. Lewis, W.T. Thompson, J. Nucl. Mater. 366 (2007) 8–27.
[9] A.F. Guillermet, G. Grimvall, J. Less-Common Met. 147 (1989) 195.
[10] D.A. Powers, High Temp. Sci. 31 (1991) 105.
[11] J. A. Rard, M. C. Amaia Sandino, and E. Osthols (Eds.). *Chemical Thermodynamics of Technetium*. North-Holland, (1999).
[12] R.J. Trainor, M.B. Brodsky, Phys. Rev. B 12 (1975) 4867.
[13] Y. Shirasu, K. Minato, J. Alloys Comp. 337 (2002) 243–247.
[14] V. I. Spitsyn, V. E. Zinov'ev, P. V. Gel'd, and D.A. Balakhovskii. Proc. Acad. Sci. USSR, Phys. Chem. Sect. 221 (1975) 225.
[15] R.J.M. Konings, W.M.P. Franken, R. Conrad, J.F. Guegnon, J.-C. Spirlet, Nucl. Technol. 117 (1997) 293–298.
[16] J.C. Lashley, M.F. Hundley, A. Migliori, J.L. Sarrao, P.G. Pagliuso, T.W. Darling, M. Jaime, J.C. Cooley, W.L. Hults, L. Morales, D.J. Thoma, J.L. Smith, J.B. Goates, B.F. Woodfield, G.R. Stewart, R.A. Fisher, N.E. Phillips, Cryogenics 43 (2003) 369–378.
[17] J. Majzlan, A. Navrotsky, B.F. Woodfield, B.E. Lang, J. Boerio-Goates, R.A. Fisher, J. Low Temp. Phys. 130 (2003) 69–76.
[18] E. Gamsjager, M. Wiessner, H. Monats, Chem. 149 (2018) 357–368.
[19] V.V. Novikov, J. Therm. Anal. Calor. 138 (2021) 265–272.
[20] A.L. Smith, R.J.M. Konings, in: Chemical Thermodynamics and Reaction Kinetics of Nuclear Materials, Woodhead Publishing, 2019, pp. 3–88.
[21] O. Benes, P. Gotcu, F. Schwörer, R.J.M. Konings, T. Fangh, Anel J. Chem. Thermodyn. 43 (2011) 651–655.
[22] J.D. Cox, D.D. Wagman, V.A. Medvedev, CODATA Key Values for Thermodynamics, Hemisphere, New York, 1989.
[23] J.G. Bunting, T. Ashworth, H. Steeple, Cryogenics 9 (1969) 385–386.
[24] W. Schnelle, J. Engelhardt, E. Gmelin, Cryogenics 39 (1999) 271–275.
[25] Q. Design, Technical Report Application Note 1085–152 (2014).
[26] P. Javorsky, F. Wastin, E. Colineau, J. Rebizant, P. Boulet, G. Stewart, J. Nucl. Mater. 344 (2005) 50–55.
[27] R.J. Trainor, G.S. Knapp, M.B. Brodsky, G.J. Pokorny, R.B. Snyder, Rev. Sci. Instrum. 46 (1975) 197–204.
[28] S.T. Sekula, R.H. Kernohan, G.R. Love, Phys. Rev. 115 (1967) 167–172.
[29] G. Kostorz and S. Mihailovich. In *Proceedings of the Twelfth International Conference on Low Temperature Physics 1970 (E. Kanda ed.)*, page 341. Academic Press of Japan, Tokyo, (1971).
[30] J. Bevk, Phil. Mag. 28 (1973) 1379–1390.
[31] J.K. Hulm, B.B. Goodman, Phys. Rev. 106 (1957) 659–671.
[32] R.R. van der Laan, R.J.M. Konings, J. Alloys Compd. 297 (2000) 104–108.
[33] J.W. Arblaster, Calphad 19 (1995) 339–347.
[34] J.W. Arblaster, Calphad 20 (1996) 343–352.
[35] J.W. Arblaster, Johnson Matthey Technol. Rev. 65 (2021) 54–63.
[36] P.D. Desai, J. Phys. Chem. Ref. Data 16 (1987) 91–108.
[37] I. Grenthe, X. Gaona, A.V. Plyanusov, L. Rao, W.H. Runde, B. Grambow, R.J. M. Konings, A.L. Smith, E.E. Moore, Second Update on Chemical Thermodynamics of Uranium, Neptunium, Plutonium, Americium and Technetium. OECD Nuclear Energy Agency, Data Bank, 2020.